# Effect of the ZnO Seed Layer Prepare three different hydrothermal growth techniques for ZnO nanorod (VI).

Mohammed N. Ali[1], Sabah A. Salman[1], Mohammed A. Dwood [2]
[1]Department of physics, College of Science, University of Diyala, Diyala, Iraq
[2]Department of physics, College of Science, University of Mustansiriya, Baghdad, Iraq
Mohammednaife123457@gmail.com ; Mohammed.N.Ali@tu.du.iq
Email: pro.dr_sabahanwer@yahoo.com

**Abstract**
ZnO nanorods (ZnO NRs) were made using physical processes, including dip-coating, evaperation, and hydrothermal. Using X-ray diffraction, the structure of ZnO NRs was investigated (XRD). To examine the absorption spectra, a UV-visible spectrometer was employed. Using (FESEM) , ZnO NRs was investigated (FE-SEM). The produced ZnO NRs have a hexagonal phase structure, according to a (XRD) research. Additionally, the ZnO NRs' average crystallite size ranged from 12.15 nanometers to 48 nanometers ( Scherrer ), respectively. The obtained ZnO nanorod samples have demonstrated nanoparticle-shape of the first prepared seedlayer by dip coating and radial hexagonal-shape of the second prepared seedlayer via hydrothermal technique, according to FE-SEM results. The estimated direct band gaps energies for the ZnO NRs' absorption spectra were 3.21 and 3.48 eV and 382 and 400 nm, respectively.
Keywords: nanorod, ZnO, evaperation, hydrothermal method

## 1. Introdution

Discussions over what makes zinc oxide (ZnO) a desirable competitor material among a variety of materials in the production of optoelectronic device applications are ongoing. ZnO possesses a straight and wide bandgap of 3.37 eV at room temperature [1], substantial piezoelectric constants [2], strong thermal conductivity [3], and room temperature mobility of 205 $cm^2$ V s [4] Large non-linear optical coefficients and a free exciton binding energy of 60 meV [5], [6], strong luminescence [7], and strong sensitivity [8], It can therefore be utilized in a variety of devices, including solar cells [9], electrodes for photoelectrochemical reactions [10], photocatalysts [11], sensors [12], piezoelectric components [13], ultraviolet laser diodes [14], and electroluminescent applications [15]. ZnO nanorods can be manufactured using solvothermal and hydrothermal processes. To create various functional oxide-film types, dip coating and sputerring techniques are frequently used. Additionally, the hydrothermal method, one of the most popular and reasonably priced techniques for the synthesis of nanometers, has been represented by the combination of metal salt and water under the influence of temperature. In this study, the structural, optical, and morphological surface characteristics of ZnO nanorods that had been generated by dip coating, hydrothermal techniques, and evaperation method were examined.

### Synthesis and characterization

Seed layer deposition is the first stage. It was applied using the sol gel-dip coating process to an FTO glass substrate. The coating's sol-gel solution was created by combining 0.2 M zinc acetate-2-hydrate [Zn (CH3COO)22H2O] and 0.2 M diethanolamine NH(CH2CH2OH)2, then stirring the mixture for 30 minutes at 60 oC to create a homogenous and colloid solution. This solution was then aged over the night. Following that, the FTO glass substrates were submerged in the ready solution to perform the dip-deposition. Finally, the ZnO nanorods underwent an hourlong annealing process at 350 oC. The hydrothermal deposition of ZnO nanorods is done in the second step. It was supported by an aqueous mixture containing 0.04 M each of hexamethylenetetramine (HMTA, C6H12N4) and zinc nitrate-6-hydrate (Zn (NO3)2.6H2O). The samples of ZnO seed layer were then submerged in the prepared combination solution for 4 hours at 90 degrees Celsius. These samples were then repeatedly rinsed in deionized water to eliminate the leftover contaminants. The ZnO NRs were then annealed for a full hour at 350 oC. Shimadzu 6000 diffractometer with CuK radiation (= 1.5406 A) at 40 kV and 40 mA was used to analyze the samples' structure and phases. Shimadzu 1800/spectra photometer was used to measure the absorbance spectra of the produced samples. It was captured between 300 and 1100 nm using plain FTO as a reference electrode. (FESEM) using a (FEI Nova NanoSEM 450) operating at (10) keV was used to determine the morphology of the samples.

## 2. Results and Discussion

### Structural Analysis

ZnO nanorod samples scanned in the 2 range between (20° and 70°) are shown in Fig. 1's XRD patterns. Many Bragg reflections are found to

doi.org/10.31838/hiv23.02.40 Received: 11.10.22, Revised: 21.11.22, Accepted: 16.12.22

originate from the produced ZnO NRs, which are more numerous. According to Table 1, the peaks seen at values of 2 correspond to the lattice plane, proving that both samples of ZnO have wurtzite hexagonal structure. All of the peaks match typical FTO glass with a cubic index, which may be indexed as having a hexagonal wurtzite structure (JCPDS card no. 003-0888). Using the Debye-Scherrer equation, D = 0.9/Cos, it is possible to determine the crystallite size (D) of the produced samples. 12.15 nm is found to be the crystallite size of processed samples.

Table 1 shows some of the X-ray diffraction data Seed Layer thin films .

| Structural parameters | | Zinc-Oxide Seedlayer | ZnO NRs by Drop Casting | ZnO NRs by Sputtering | ZnO NRs by Evaporation |
|---|---|---|---|---|---|
| $D_{av}$ (nm) | Scherrer | 43.11 | 12.15 | 48 | 43.92 |
| | W.H | 40.78 | 10.96 | 47.89 | 41.89 |
| ($\delta$) *$10^{-4}$ ($nm^{-2}$) | Scherrer | 5.38 | 67.74 | 4.43 | 5.18 |
| | W.H | 7.33 | 82.64 | 4.36 | 5.68 |
| Micro Strain ($S$) *$10^{-3}$ | | -6.32 | -12.46 | +0.995 | -6.66 |

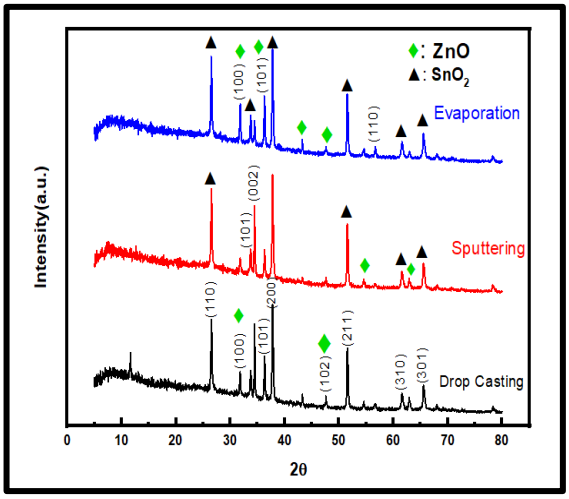


*Figure 1. XRD patterns ZnO nanorod (a) Evaporation (b) Sputtering (c)Drop casting.*

## UV-Vis spectral analysis

ZnO NRs' UV-Vis absorption spectra are shown in the Figure 2. The optical absorption edge of ZnO NRs, which is discovered at about 382 nm and 400 nm, is shown. According to Fig. 2, the ZnO nanorod's estimated band gap is 3.21 eV, which is a little different from the ZnO NRs (3.48 eV). As a result, ZnO NRs are superior to nanoparticles in terms of surface area and optical and conducting qualities. This makes the geometry of nanorods particularly helpful in a wide range of applications.

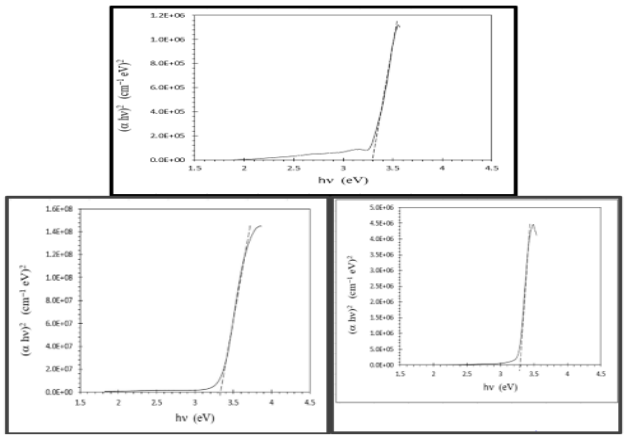


*Figure 2 shows the UV-Vis spectra and band gap energy curves of ZnO nanorods produced by the following processes: (a) evaporation (b) sputtering (c) drop casting.*

## 3. Morphology Analysis

The surface morphology of the pure ZnO nanoparticles that were obtained in a homogeneous surface morphology was examined using FE-SEM in Fig. 3. after growth of the ZnO NRs demonstrates how the particles' radial hexagonal forms are independently separated. The inset of Fig. 3 demonstrates that the typical diameter of nanorods is ~ 90 ± nm.

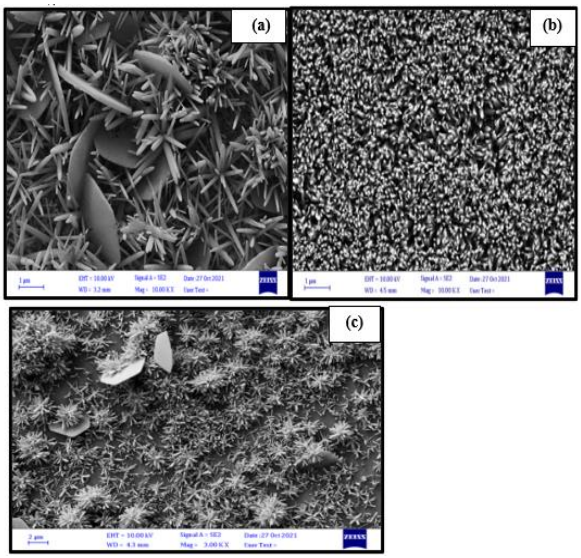


*Figure(3). Images of the ZnO nanorod after (a) evaporation, (b) sputtering, and (c) drop casting taken with a field emission scanning electron microscop*

## 4. Conclusion

ZnO nanorods, which have a wide range of uses, were created in the current work. According to Scherrer, ZnO nanorods have average crystallite sizes of 12.15 nm, 43.11 nm, 43.92 nm, and 48 nm, respectively, and are in the hexagonal phase. ZnO NRs samples' optical absorption edges were feasible between the wavelengths of 382 and 400 nm. For ZnO nanorod, it was discovered that the calculated optical band gaps were 3.21 eV and 3.48 eV, respectively. The surface morphology was examined using FE-SEM analysis, and the resulting image

shows that the nanorods are independently separated from the ZnO nanoparticles and have radial hexagonal forms.

## References

[1] Dong H, Zhou B, Li J, Zhan J, Zhang L 2017 Ultraviolet lasing behavior in ZnO optical microcavities Journal of Materiomics 3 255-266.
[2] Molarius J, Kaitila J, Pensala T, Ylilammi M 2003 Piezoelectric ZnO films by RF sputtering Journal of Materials Science: Materials in Electronics 14 431-435.
[3] Florescu D I, Mourokh L G, Pollak F H, Look D C, Cantwell G, Li X 2002 High spatial resolution thermal conductivity of bulk ZnO (0001) Journal of applied physics 91 890-892.
[4] Look D C, Reynolds D C, Sizelove J R, Jones R L, Litton C W, Cantwell G, Harsch W C 1998 Electrical properties of bulk ZnO Solid state communications 105 399-401.
[5] Bagnall D M, Chen Y F, Shen M Y, Zhu Z, Goto T, Yao T 1998 Room temperature excitonic stimulated emission from zinc oxide epilayers grown by plasma-assisted MBE Journal of crystal growth 184 605-609.
[6] Larciprete M C, Haertle D, Belardini A, Bertolotti M, Sarto F, Günter P 2006 Characterization of second and third order optical nonlinearities of ZnO sputtered films Applied Physics B 82 431437.
[7] Shionoya S and Yen W H (ed) 1997 Phosphor Handbook By Phosphor Research Society (Boca Raton, FL: CRC Press).
[8] Nanto H, Sokooshi H and Usuda T 1991 Smell sensor using zinc oxide thin films prepared by magnetron sputtering Solid-State Sensors and Actuators 596-599.
[9] Zhou C, Ghods A, Yunghans K L, Saravade V G, Patel P V, Jiang X, Ferguson I 2017 ZnO for solar cell and thermoelectric applications. In Oxide-based Materials and Devices International Society for Optics and Photonics 10105 101051K.
[10] Mohd Fudzi L, Zainal Z, Lim H, Chang S K, Holi A 2018 Effect of Temperature and Growth Time on Vertically Aligned ZnO Nanorods by Simplified Hydrothermal Technique for Photoelectrochemical Cells Materials 11704.
[11] Ong C B, Ng L Y, Mohammad A W 2018 A review of ZnO nanoparticles as solar photocatalysts: Synthesis, mechanisms and applications Renewable and Sustainable Energy Reviews 81 536-551.
[12] Wei A, Pan L, Huang W 2011 Recent progress in the ZnO nanostructure-based sensors. Materials Science and Engineering: B 176 1409-1421.
[13] Bhatia D, Sharma H, Meena R S, Palkar V R 2016 A novel ZnO piezoelectric microcantilever energy scavenger: Fabrication and characterization. Sensing and bio-sensing research 9 45-52.
[14] Liu C Y, Xu H Y, Sun Y, Ma J G, Liu Y C 2014 ZnO ultraviolet random laser diode on metal copper substrate Optics express 22 16731-16737.
[15] Zhang S G, Zhang X W, Yin Z G, Wang J X, Dong J J, Wang Z G, Chow P P 2011 Improvement of electroluminescent performance of n-ZnO/AlN/p-GaN light-emitting